ISSN 0252-1075
Contribution from IITM
Research Report No. RR-104

Initialization Experiments over Indian Region with a Limited Area Model using Recursive Digital Filters

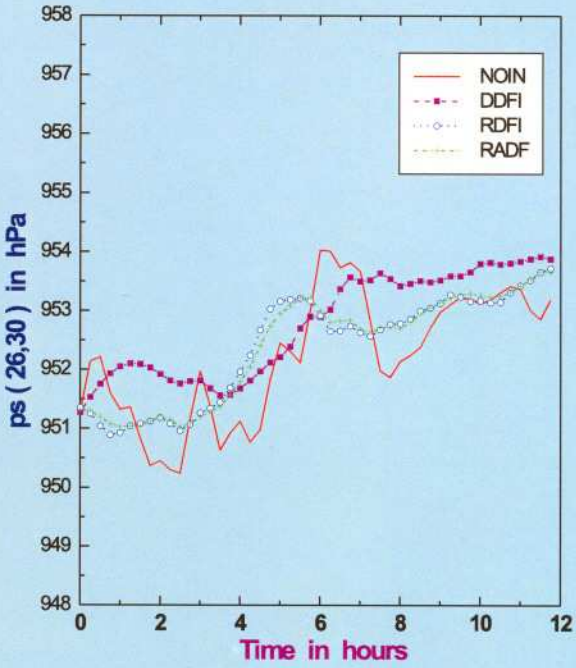

A. Bandyopadhyay
and
S. Mahapatra

July 2004

Indian Institute of Tropical Meteorology
Pune - 411 008, India

ISSN 0252-1075
Contribution from IITM
Research Report No. RR-104

Initialization Experiments over Indian Region with a Limited Area Model using Recursive Digital Filters.

A. Bandyopadhyay
and
S. Mahapatra

July 2004

Indian Institute of Tropical Meteorology
Dr. Homi Bhabha Road, Pashan Pune - 411 008
Maharashtra, India

E-mail : lip@tropmet.ernet.in
Web : http://www.tropmet.ernet.in
Fax : 91-020-25893825
Telephone : 91-020-25893600

CONTENTS

Initialization Experiments Over Indian Region With a Limited Area Model Using Recursive Digital Filters.

A. Bandyopadhyay and S. Mahapatra

Indian Institute of Tropical Meteorology,
Dr. Homi Bhabha Road, Pashan,
Pune - 411008, India.

Abstract

Two versions of recursive digital filtering initialization (DFI) schemes have been applied to a limited area model to examine their impact on the model performance on short - range prediction over Indian region. For comparison, the input is also initialized by non - recursive diabatic digital filtering initialization (DDFI) technique. It is found that both the versions of recursive filter could produce fairly well - balanced initial state and could effectively suppress the high frequency oscillations from the forecasts. The filters are found to be more effective in controlling the noise in the first few hours of integration. The changes induced to the analysis by both the versions of recursive filters are reasonably small and are comparable with changes made by non - recursive filter (DDFI). The 24 hr forecasts from the either of the two recursive DFI schemes are comparable with those produced from DDFI scheme and also with the forecasts obtained from uninitialized input. The main advantage of DFI is found to be its great simplicity in conception and application. Its implementation is very easy, requiring only the calculation of the filter coefficients and minor adjustments of the model code.

1. INTRODUCTION

In numerical weather prediction (NWP) based on primitive equations, the unrealistically large-amplitude high frequency inertia gravity-wave oscillations occur in the forecasts if the initial mass and wind fields are not in a proper state of dynamical balance with each other. Initialization is a procedure through which the initial mass and wind fields are brought to a state of balance which, in turn, leads to a smooth and noise free forecast. Many initialization schemes viz. static and dynamic initializations, linear and non - linear normal mode initialization, dynamic normal mode initialization, physical initialization, DFI etc. have been proposed. Amongst these, the DFI, formulated by Lynch (1990) is, perhaps, the latest.

The DFI technique, based on digital filters, are of two types, viz, non-recursive and recursive and can be applied adiabatically as well as diabatically. The filter operates on a time series of dependent variables produced by adiabatically backward and adiabatically or diabatically forward short - range integration of the forecast model. The filter removes the high-frequency noise from the time - series. A balanced initial state is thus achieved through the adjustment of all the dependent variables of the model. Lynch and Huang (1992) have applied non - recursive adiabatic DFI technique (ADFI) to initialize a high -resolution limited area model (HIRLAM). Huang and Lynch (1993) have extended ADFI to include diabatic processes and formulated a non - recursive DDFI procedure and once again successfully implemented in HIRLAM.

The initialization technique based on non - recursive filter, though, has been found to give satisfactory results, has inherent disadvantage. In case of DDFI with diabatic processes a backward adiabatic integration of the model for half the filter - span starting from the original analysis at time $t = 0$ is carried out. The backward integration is required in order to make the filtered output valid at the original analysis time (at the center of the filter-span). Then using the model state at the end of backward adiabatic run, a forward diabatic integration is to be carried out for full filter - span. This backward integration is the demerit of non - recursive DDFI procedure, since the forward diabatic trajectory starting from the end of backward run, generally, does not pass through the initial data at time $t = 0$. Thus a backward integration followed by a forward run means we are filtering the values on a trajectory that does not pass through the original analysis at $t = 0$. A number of modifications were suggested and tested to alleviate this short - comings of non - recursive DDFI scheme but without much success. Ideally, a balance initial state deduced from a forward diabatic trajectory starting from the original analysis at time $t = 0$ should be used. Lynch (1993a) have demonstrated that this could be achieved by means of recursive filter (defined in Sec. 3), which, unlike non - recursive filter, allows the feed back of the previous filtered output values. A straight - forward application of a recursive filter to a one - sided forward trajectory can produce a fairly well - balanced initialized fields that allow a noise free integration but yield the filtered output valid at somewhat later than the original analysis time. This means that a recursive filter, when applied to an one - sided trajectory, causes a phase shift which, in turn, makes

the changes in analysis and forecasts very large. Lynch (1993 a) proposed several alternative formulations such as recursive diabatic filtering (RDFI), recursive adiabatic - diabatic filtering (RADF), recursive incremental filtering (RINF), recursive incremental adiabatic- diabatic filtering (RIAD) etc. to allow for this discrepancy. Lynch (1993 a) have further shown using the HIRLAM model, that all those versions of recursive filtering scheme, when applied in a non - recursive way, are very effective in reducing the phase - shift associated with the recursive filters without causing or inviting any penalty in computer time or storage as compared to the non - recursive filter. In the present study, authors have applied two different versions of recursive digital filtering (RDF) initialization schemes following Lynch (1993a) to a limited area model to examine their impact on the short - range forecast performance of the model over Indian region. The two versions of RDF used are RDFI and RADF. Two more parallel model integration are carried out. In one case the integration starts from the un-initialized data (hereafter referred to as NOIN experiment) and it provides one of the references to which the RDFI and RADF experiments are compared. In the second parallel run, input is initialized by non - recursive DDFI scheme following Huang and Lynch (1993) and will serve as the second reference for comparison with performance of recursive filters.

The layout of the remainder of the paper is as follows. In Section 2., we briefly describe the model and the data used in this study. The design of recursive filter and its application for initialization are presented in Section 3. The results of numerical experiments are summarized in Section 4 followed by the concluding remarks in Section 5.

2. MODEL DESCRIPTION, DATA AND SYNOPTIC SITUATION

2.1 Model

The forecast model used in this study is adopted from Florida State University ' s (FSU) limited area primitive equations grid - point model formulated on a rectangular Cartesian co - ordinate system in which sigma σ (= p/p_s, p is the pressure at any level and p_s is the surface pressure) is used as is vertical coordinate. The horizontal wind (u, v), temperature (T), specific humidity (q) and the surface pressure (p_s) are the prognostic variables These time - dependent variables are staggered on Arakawa C - grid. The model uses a staggered arrangement of variables in vertical also. Among the vertically dependent variables, the height (z) and the vertical velocity ($\dot{\sigma}$) are defined at interfaces. All other variables u, v, T and q are set at the middle of each layer. The governing equations involved are the zonal (u) and meridional (v) momentum equations, thermodynamic equation for T, moisture continuity equation for q, mass continuity equation in terms of surface - pressure ps, hydrostatic relation for obtaining z diagnostically and the equation of state. The virtual effect of moisture on temperature is taken into account. The model physics includes short- and long - wave radiation, shallow convection, deep cumulus convection (Kuo - type convective scheme), large - scale condensation, horizontal and vertical diffusion of momentum, sensible heat and moisture. The details of parameterization of these physical processes have been documented by Arun Kumar (1989).

The model has nine levels in vertical between the top (σ =.1) and the bottom (σ = 1. 0) with a uniform spacing of 0.1 ($\Delta\sigma$). In vertical the air parcels are not allowed to cross the upper and lower boundaries. Rigid boundary conditions are, therefore, imposed by setting $\dot{\sigma} = 0$ both at the upper and lower boundary. Since the model is a limited area model, a lateral boundary condition must be specified. A sponge-zone over a specified distance, spanning over five points from the lateral boundaries is specified in order to gradually blend the predictive variables with their observed values. By the time lateral boundaries are reached the observed values are imposed. Throughout the rest of the grid (free zone), the predicted values are not affected by the observed values. The forecast value of a variable at time $t + \Delta t$ and located within the sponge - zone is then modified as

$$X_m = Xp(x, y, \sigma) + \alpha[X_R (x, y, \sigma) - X_p(x, y, \sigma)] \qquad \ldots (1)$$

where, α is a weighting factor which varies from 0 in a free-zone to a value 1 at the lateral boundaries, X_p stands for the model predicted value of X, X_R the observed value and X_m modified value. The above nudging of two fields is applied at all σ - levels in vertical and at each time - step of model integration and on u, v, z, q and p_s. It should be mentioned that the boundary condition (1) is applied while producing the actual forecast. When the model is integrated for initialization purpose, the boundary values of the variable are not allowed to vary with time.

For producing forecast as well as for initialization purpose, the time - integration of the model is carried out with two - time level (one-step) Semi - Lagrangian Semi - implicit scheme (Arun Kumar,1989).

2.2 Data and synoptic situation

In the present study input to the model is of 12 UTC, 7 July, 1979 data. In addition to this, 00 UTC of 8 July, and 12 UTC of 8 July, 1979 were also required for boundary updating and validation purpose. All these data are extracted from ECMWF-FGGE level IIIb data set. These globally analysed data available at 1.875° resolution and at 15 standard pressure levels in vertical are interpolated to the model grid - points and at model ' s sigma levels. The complete interpolation procedure is carried out in two steps. First the variables are interpolated horizontally to the model grid using bilinear technique but still at 15 pressure levels. In second step, those provisionally interpolated values at model ' s grid are then interpolated vertically at the model ' s sigma levels using cubic spline technique.

The prevailing synoptic situation during those days over the domain of interest was a monsoon depression over north Bay of Bengal and the adjoining areas. On 4 July, a low formed over the head Bay of Bengal with its center at about 20° N and 90° E. The low - pressure system intensified into a depression (mature stage) on 7 July and moved slowly north-westerly direction and crossed the Indian coast near Paradip in Orissa on 8 July and then weakened on 9 July and subsequently dissipated.

3. THEORY, DESIGN AND IMPLEMENTATION OF RECURSIVE FILTER

3.1 Theory and design

Let us consider a function f (t) of time t consisting of low and high frequency components. Further, we consider that f (t) is known at discrete moments $t_n = n \Delta t$ at a time interval of Δ t. That is, the sequence f_n is known for n =.... -2, -1,0, 1, 2, 3,.... We also write f (t) as $f(t) = f(t_n) = f(n \Delta t) = (f_n)$ only. For the discrete function (f_n), a non - recursive digital filter is defined as

$$y_n = \sum_{k=-N}^{N} a_k f_{n-k} \qquad \ldots (2)$$

and a recursive filter of order N is defined as

$$y_n = \sum_{k=0}^{N} a_k f_{n-k} + \sum_{k=1}^{N} b_k y_{n-k} \ldots (3)$$

For non - recursive filter, the output depends on both past and future values of f, but not on any other output values. For a recursive filter, output depends on past and present values and also on the previous filtered output values. The recursive filter is more powerful than non - recursive ones but can be more problematic as the feed - back of the previous output can give rise to instability. The response of a non - recursive filter for an initial impulse at n = 0 vanishes for n > N where as the response of a recursive filter to an initial impulse input can persists indefinitely.

To investigate the frequency response of either a non -recursive or of a recursive filter, we assume an exponential type of input, that is, we assume

$$f(t) = \exp(i\omega t) \qquad \ldots (4)$$

where ω is the frequency. In discretized form, (4) can be written as

$$f_n = \exp(in\theta), \qquad \ldots (5)$$

where $\theta = \omega \Delta t$ is the digital frequency. We further assume an output in the form of

$$y(t) = H(t) * \exp(i\omega t) \qquad \ldots (6)$$

or, in discretized form,

$$y_n = H(\theta) \exp(in\theta) \qquad \ldots (7)$$

where H (t) or H (θ) is called the transfer function or response function of the filter. On defining z = exp (iθ) the above input (5) and the output (7) can be written as

$$f_n = z^n \qquad \ldots (8)$$

and

$$y_n = H(z) * z^n \qquad \ldots (9)$$

For practical implementation of recursive filter, one has to treat the filter (3) as a difference equation of order N as

$$y_n - \sum_{k=1}^{N} b_k y_{n-k} = \sum_{k=0}^{N} a_k f_{n-k} \qquad \ldots (10)$$

Restricting ourselves to a second order filter, for which N = 2, the equation (10) can be written as

$$y_n - b_1 y_{n-1} - b_2 y_{n-2} = a_o f_n + a_1 f_{n-1} + a_2 f_{n-2}$$
$$= F_n \text{ (say)} \qquad \ldots (11)$$

The complete general solution of the above difference equation will be of the form $y_n = y^T + y^F$ where $y^T = C_1 z_1^n + C_2 z_2^n$ is the solution associated with the corresponding homogenous form of the equation (11), called the transient solution and the other part $y^F = H z^n$ is the particular solution (or the forced solution) due to the forcing F_n. C_1 and C_2 are two constants to be determined from starting values y_o and y_1 which must be supplied. For practical application for initialization, we are interested in the forced response and will, therefore, discard the transient component by setting $C_1 = C_2 = 0$. On the values of C_1 and C_2 so chosen, the general solution reduces to

$$y^n = y^F = H z^n. \qquad \ldots (12)$$

Substituting (12) in (11), we obtain

$$H = (a_o + a_1 z^{-1} + a_2 z^{-2}) / (1 - b_1 z^{-1} - b_2 z^{-2}) \qquad \ldots (13)$$

Our primary aim is to determine the transfer function H from (13) which, in turn, will give the filter output from (12) when the input z^n is known. To find H, one has to obtain a_o, a_1, a_2, b_1 and b_2 and this is exactly what is needed for implementation of recursive filter for initialization The procedure for determining those coefficients has been described in details by Lynch (1993a) and will, therefore, not be repeated here. For a second order, prototype, quick - start filter (whose transient response decays rapidly) of the form (10), Lynch (1993 a) have deduced the filter coefficients as

$$a_o = a_1 / 2 = a_2 = \mu_c^2 / (1 + \sqrt{2}\mu_c + \mu_c^2),$$

$$b_1 = 2 (1 - \mu_c^2)/ (1 + \sqrt{2}\mu_c + \mu_c^2) \text{ and} \qquad \ldots (14)$$

$$b_2 = - (1 - \sqrt{2}\mu_c + \mu_c^2)/ (1 + \sqrt{2}\,\mu_c + \mu_c^2)$$

where

$$\mu_c = \tan (\theta_c / 2) \text{ with } \theta c = \omega_c \Delta t = 2 \pi \Delta t / \tau_c. \qquad .. (15)$$

ω_c is the cut off frequency of the prototype analog filter ; θ_c and τ_c are respectively the cut off frequency and cut - off period of the transformed digital filter. Δ t is the time - step of model integration For practical application of the filter, one more parameter, the filter span (τ_s) is needed. These parameters jointly determine the characteristic of the initialization scheme using recursive digital filter. The meanings and definitions of these physical parameters are given by Lynch (1993a) and are also available in any standard book on Digital Signal processing and hence will not be redefined here.

3.2 Practical implementation and generation of filtered data

In the experiments described in this paper, second order quick - start recursive filter of type (2) has been applied to a time - series of the model out - put produced by short - range integration of the model over the period of τ_s (the total filter span) = 2 hours with a time - step (Δ t) of 360 seconds. The value used for the parameters are τ_c = 12 hrs, τ_s = 2 hrs. On the basis of values of the parameters so chosen and following the methodology of Lynch (1993a), we obtain the values of the filter coefficients as follows :

$$a_o = .00567,\ a_1 = .01134,\ a_2 = .00567$$

$$b_1 = 1.69881 \text{ and } b_2 = - 0.72149$$

In practical application the filter (2) is applied in a non - recursive manner. If we define the input and the filtered output vectors at the end of each time - step of integration up to

2 hours (so that, $\tau_s = M \Delta t = 2$ hours and M = 20) as $\mathbf{X} = (x_1, x_2, x_3, \ldots x_M)^T$ and $\mathbf{Y} = (y, y_2, y_3, \ldots y_M)^T$ respectively, then the filter (2) can be written in the matrix form as

$$\mathbf{Y} = \mathbf{AX} + \mathbf{BY} \qquad \ldots (16)$$

where **A** and **B** are lower triangular matrices. The above equation can be rewritten as

$$\mathbf{Y} = (\mathbf{I} - \mathbf{B})^{-1} \mathbf{AX} = \mathbf{FX} \text{ (say)} \qquad \ldots (17)$$

The last row of the above equation gives an expression for the output Y at the end of full filter - span $t = \tau_s = M \Delta t = 2$ hrs in terms of the input $x_1, x_2, \ldots\ldots, x_M$. For an N^{th} order filter, in general, the filtered output value at the end of each step $t_n = n \Delta t$ (n = 0, 1,.....M) can be written as

$$Y_{nk} = \sum_{k=0}^{N} F_{nk} Xn, \text{ (} n = 0, 1, 2, \ldots M \text{)} \qquad \ldots (18)$$

To generate filtered data through either of RDFI or RADF scheme, the filter is applied in the form of (18). For producing RDFI data, a forward diabatic integration of the model is performed for $\tau_s = 2$ hrs. and then the filter is applied to the time series of the predicted variables to accumulate the sum. The procedure is applied independently to each variable, at each grid point and at all the model's levels. For initialization purpose, the integration is done with a time - step (Δt) of 360 seconds. For marching forward in time for actual forecast, Δt = 900 seconds is used although, the numerical time - integration scheme mentioned in Sec.2 permits much larger value. RADF scheme, however, needs two model integrations ; a backward followed by a forward run. First, the model is integrated adiabatically backward for 1 hr. Then filter (18) is applied on the backward trajectory to estimate the sum. Using the filtered value obtained at the end of the backward run as the initial state, a forward diabatic integration is carried out for full filter - span $\tau_s = 2$ hrs. and once again the filter is applied on the forward diabatic trajectory to yield the sum of right - hand - side of (18). The final summed up value is our initialized field assumed to be valid at the initial analysis time t = 0. From the application point of view, the procedures RADF and DDFI appears to be very similar. However, there is a difference between the two. The purpose of backward integration in DDFI is to make the forward trajectory to be centered at the initial time, whereas in RADF scheme, backward run is done only to minimize the phase - shift associated with the recursive filter due to its delay characteristics.

4. NUMERICAL EXPERIMENTS AND RESULTS

As stated earlier, the primary goal of this study is to examine the impact of RDF on the model forecast performance. To this end, four different sets of 24 hr forecasts are produced over the Indian region spanning from 12° S to 35° N and 50° E to 110° E and containing 61×48 grid points with $1^{\circ} \times 1^{\circ}$ latitude - longitude horizontal resolution. Two sets of forecasts are produced starting from two different initialized data generated through two different versions of recursive filtering scheme, namely, RDFI and RADF. The third forecast is obtained from the non - recursive DDFI scheme and the fourth set of forecast are computed from the un-initialized (NOIN) data. The impact of RDF on the model forecast performance is assessed by comparing the RDFI and RADF forecasts with NOIN as well as with DDFI forecasts. The individual performance of RDFI and RADF are also examined in the light of the three essential requirements for any initialization scheme. These are (i) the changes made in the initial data due to initialization should be reasonably small, (ii) the forecast produced from the initialized fields should not be degraded as compared to the forecasts obtained from the un-initialized analysis and (iii) the spurious high -frequency noise is eliminated from the forecast.

4.1 Changes made in the original analysis due to initialization.

To examine the changes induced in the original analysis due to different initialization schemes, the maximum difference (MAXD) and the root mean square (RMS) difference in the horizontal wind components (u, v), temperature (T) and surface - pressure (p_s) between the initialized and un-initialized fields are computed and presented in Table 1. It can be seen that the changes made in the observed analysis by all the initialization schemes DDFI, RDFI and RADF are reasonably small. The MAXD induced by RDFI in the analysis for all the parameters u, v, T and p_s are more as compared to the changes made by DDFI and RADF. The change in p_s induced by DDFI is minimum and maximum in RDFI scheme. However in all the schemes, changes are of the same order of magnitude. Same is the case for RMS changes. The RMS changes made by RDFI are somewhat larger than those induced by both DDFI and RADF and this is true for the all the variables including p_s. Comparison of RMS between DDFI and RADF shows that for u and v, the changes are comparable and for T and p_s the changes by DDFI are marginally smaller.

The mean sea level (MSL) pressure maps for all the four sets of input (NOIN, DDFI, RDFI and RADF) are shown in Fig.1 which reveals that all the four maps closely resemble each other. The closed isobar of minimum pressure 994 hPa around the center of the depression shown by each of the three initialized charts is absent in NOIN map which depicts the minimum pressure of 996 hPa around the center. Another closed and elongated isobar of 994 hPa in the north - western sector is well - marked in all three initialized as well as uninitialized maps. However, in both the versions of recursive

filtering, the isobar is closed whereas it is seen as broken cells in both DDFI and NOIN cases. The spatial distribution as well as the magnitudes of the isolines representing the high - pressure regions at the north - eastern part of the domain are very similar in all the initialized data as well as in NOIN data.

4.2 Changes made in the forecast by initialization

To examine the changes made in the forecasts by DDFI, RDFI and RADF as compared to NOIN, the RMS and MAXD values are computed for u, v, T and p_s between the 24 hr forecast fields obtained from the three initialized inputs and the uninitialized analysis. These statistics, presented in Table 2, reveal that the RMS and MAXD values for all the parameters between NOIN and each of the three initialized forecasts are reasonably small. In general, the changes (both in RMS and MAXD) by DDFI scheme are higher than the changes made by each of the two recursive initialization schemes. The changes in RMS values by RADF are marginally smaller than the changes made by RDFI. A comparative look on the Tables 1 and 2 shows that the RMS changes made to the 24 hr forecast for all the four variables u, v, T and p_s by each of the initialization scheme are marginally smaller than the respective changes induced by them in the original analysis. That the RMS changes in forecasts by RDFI as well as by RADF are very small, indicates that the recursive filters did not affect the forecast very much if the un-initialized forecast is used as reference. Moreover, the smaller values of RMS by both the recursive filters compared to the DDFI also explains the fact that both RDFI and RADF forecasts are closer to the un-initialized forecast than DDFI forecast.

To further assess the impact of recursive filtering schemes on the model forecast performance as compared to DDFI and NOIN forecasts, the spatial distribution of 24 hr. forecasts of MSL pressure field produced from each of the three sets of initialized input as well as from NOIN analysis are examined and presented in Fig. 2 along with the observed map of 1200 UTC, 8 July, 1979 (for verification). It can be seen that the general patterns of forecast MSL pressure distribution obtained from any of the four sets of input are close to each other. Each of the three initialized forecasts agrees well with the observed pattern as well as with the NOIN forecast with the exception that the closed isobar of lowest pressure of 994 hPa found in the observed chart is not properly simulated by the model with any of the three sets of input nor with the un-initialized analysis. The observed isobars of high - pressure like 1008, 1010, 1012 and 1014 hPa in the north-eastern part of the domain are well predicted by the model almost in same fashion with any of the four sets of input data. This aspect reflects the property of any initialization scheme (mentioned in the beginning of Sec. 4) that initialized forecast should not be inferior as compared to the un-initialized one.

Fig.3 depicts the forecast geo potential height at 850hPa, produced from all the four sets of input, along with the observed map of 12 UTC, 8 July. All the four forecasts produced either from NOIN analysis or from digitally filtered data, recursively or non -

recursively, are seen to be very similar with each other. Overall forecast pattern appears to be close to the observed with the marginal difference at the center of the depression. The observed contour at the center of the system is of the order of 1400 m or less which is not properly predicted by the model with un-initialized data nor with any of the three initialized input. The forecasts also differ with respect to the observed near the north - eastern (NE) part of the domain. The model predicted high pressure region in NE part, with any of the four sets of input and represented by the closed contour as high as 1510 m is absent in the actual. The very close resemblance is also seen in all the forecasts wind (not presented) which are again found to be very similar to the observed.

4.3 Reduction of high - frequency noise

The basic purpose of any initialization scheme is to eliminate the high - frequency oscillations from forecast. A common practice for measuring the noise level in the forecast is to examine the oscillations of mean absolute surface pressure tendency (MASPT) as the time - integration proceeds Another way of measuring the noise - level is to examine the time variation of surface - pressure (ps) itself. The evolution of ps at a model grid - point in first 12 hrs of forecast produced from all the four sets of input is depicted in Fig. 4 which shows that ps oscillates noisily during the un-initialized run and this indicates severe contamination of forecast by high - frequency noise in NOIN case. This is due to the presence of imbalance between mass and wind fields in the NOIN data. That the noise level in all the three initialized runs is removed considerably is evident from the fact that the amplitudes of high - frequency oscillations in the initialized forecast - curves are significantly reduced. Though the residual high - frequency noise is still there in all the three initialized cases, the noise level is considerably less compared to the NOIN run. The distinct difference between the NOIN and the three initialized curves clearly shows that the initial imbalance between the mass and wind field of NOIN data is effectively controlled and reduced to a great extent by both the versions of recursive filters (RDFI and RADF) as well as by the non - recursive filter (DDFI). The Fig. 4 also depicts that of the two filtering methods, the reduction of noise - level is less by DDFI scheme than by both the versions of recursive filter, at least in the first few hours of integration. Of the two recursive versions, noise control seems to be comparable. An interesting conclusion from the Fig. 4 is that the large amplitude high - frequency oscillations in NOIN forecast decreases as the length of the forecast increases. This may be due to the inherent built - in damping processes (smoother, filter etc) in model. Another aspect found is that all the curves almost coincide with each other after 12 hrs of integration and thereafter display very close and fairly steady run. This indicates that the forecast results show very little high-frequency oscillations after 12 hrs even in NOIN case and that is why the results are presented only up to 12 hrs in Fig. 4.

While the surface - pressure (p_s) is sensitive to vertically integrated sense and its time variation is a good indicator of external noise, the variation of vertical velocity reflects the internal noise. The Fig. 5 presents the time - evolution of vertical velocity

($\omega = dp / dt$) at level 7 ($\approx$ 700 hPa) of the forecast model and at the same grid - point for the first 12 hrs of forecast obtained from each of the four sets of input. The Fig. 5 shows a good agreement with results of the Fig. 4 The Fig. 5, like p_s, once again shows high - frequency oscillations in NOIN forecast indicating imbalance of mass and wind fields in the un-initialized analysis. The reduction of noise, to a great extent, is clearly seen in all the initialized runs. The reduction of noise level by both RDFI and RADF schemes, like in case of ps, seems to be very close to each other in the entire length of forecast.

5. CONCLUSIONS

The impact of recursive DFI procedure on short - range forecast performance of a limited area model over Indian region has been investigated. For this, two different versions, viz, RDFI and RADF are implemented. For comparison, a third set of initialized data is also produced through non - recursive DDFI scheme. The forecast performance of the two recursive filters are evaluated by comparing the model forecasts produced from them with the forecasts obtained from DDFI data as well as from NOIN input. The RDFI and RADF are found to have generated well - balanced and synoptically well- organized model initial state that led to a smooth integration of the model. The initialized input from both RDFI and RADF are found comparable with DDFI generated data. Changes induced in the original analysis by all the three schemes are reasonably small and are of the same order of magnitude. The changes made in 24 hr forecast fields by all the schemes are also small. However, the forecast statistical values (RMS and MAXD), in general, are little larger in DDFI as compared to the values in RDFI and RADF. The forecast MSL pressure pattern produced from RDFI and RADF data are very close to each other and are very similar with the forecast MSL field obtained from DDFI data as well as from NOIN input. This indicates that recursive DFI procedure, when applied over Indian region to initialize data for numerical model, could preserve all the essential characteristics that any initialization technique (mentioned in Sec. 4) should have.

There is no significant improvement in the overall forecasts obtained from any of DDFI, RDFI or RADF data over NOIN forecasts. This is probably because the model has built-in damping processes such as smoother and filter. Those smoother and filter suppress the growth of high - frequency noise in un-initialized forecasts and at the end of 24 hrs of integration, a smooth forecast field appears even without initialization and therefore, NOIN forecasts are found comparable with all the three initialized forecasts. However, it should be mentioned that both versions of recursive filter have shown significant impact in the beginning of the forecast with respect to NOIN forecast. This impact can be seen from Figs. 4 and 5 which suggest clearly that both RDFI and RADF could effectively control the high - frequency noise at least, in the first few hours of integration.It should be also mentioned that neither of the two versions of the recursive filters could produce overall 24 hr forecasts better than the forecasts generated by DDFI input. The forecasts from RDFI, RADF and DDFI data are more or less identical. The

reason probably lies in the delay characteristic associated with recursive filters which causes the filter output to be valid at a time somewhat later than the original analysis time (t = 0). In the present experiments with either of the two versions of recursive DFI schemes, the filter is applied only once during entire filter span τ_s. It appears that though the single application of the filter has eliminated the high - frequency noise sufficiently, but could not reduce the phase - shift significantly. One means to reduce the phase - error is to apply the filter iteratively using the final output of one iteration as the input for the next one and so on but with the same input each time. Another approach to minimize the phase - difference is to apply the filter only to analysis increment and not to the analysis itself. A third alternative is to use higher order filter ($N \geq 3$). However, none of the three alternative have been attempted in the present experiment and are left for future study. Finally, we conclude that our primary objective was to have a balanced, free of high - frequency noise and synoptically well organized initial input which would lead us to a smooth and noise free integration of the model. From that point of view, we infer that recursive digital filters have served the purpose and encouraged the authors to carry out the alternative experiments mentioned above.

6. ACKNOWLEDGEMENTS

The authors wish to thank Dr. G. B. Pant, Director, Indian Institute of Tropical Meteorology, Pune, for his interest and for providing the necessary facilities to carry out this study. Authors are also thankful to Shri P. Seetaramayya, Head of Forecasting Research Division, for his encouragements.

7. REFERENCES

Arun, Kumar., 1989. Documentation of FSU limited area Model (USA), FSU Report No. 89-4

Arakawa, A., and Lamb, V. R, 1977. Computational design of basic dynamical processes of the UCLA general circulation model. Math. Comp. Phys (Academic press,USA)., 17, 173 - 265

Huang, Xiang - Yu. and Lynch, P. 1993., Diabatic digital filtering initialization : Application to HIRLAM model. Mon. Wea. Rev., 121, 589 - 603.

Lynch, P.,1990. Initialization using digital filter. Research activities in atmosphere and ocean modeling. CAS/JSC working group on numerical experimentation. Report No. 14, WMO secretariat, Geneva, 1.5 - 1.6

Lynch, P. and Huang, Xiang - Yu., 1992. Initialization of The HIRLAM model using a digital filter. Mon. Wea. Rev., 120, 1019 - 1034.

Lynch, P., 1993a. Digital filters for numerical weather prediction. HIRLAM Technical Report No. 10. Meteorological service, Dublin, Ireland.

TABLE – 1

Root Mean Square (RMS) and Maximum difference (MAXD) in horizontal wind components (u and v in m / sec), temperature(T in degree Kelvin) and surface pressure (ps in hPa) between the initialized and un-initialized analyses. For u, v and T, the statistics are for three dimensional domain.(DDFI - NOIN) : Changes induced by DDFI on NOIN data ; (RDFI - NOIN) : Changes made by RDFI scheme on NOIN fields and (RADF - NOIN) : changes made by RADF technique on NOIN data.

	RMS				MAXD			
	u	v	T	p_s	u	v	T	p_s
DDFI - NOIN	0.50	0.60	0.18	0.60	3.70	4.10	1.60	2. 20
RDFI - NOIN	0.62	0.60	0.22	1.30	5.70	5. 40	1.60	4. 00
RADF-NOIN	0.50	0.50	0.19	1.10	3.10	3.10	1.30	2.50

TABLE – 2

Root Mean Square (RMS) and Maximum difference (MAXD) in horizontal wind components (u and v in m / sec), temperature (T in degree Kelvin) and surface pressure (ps in hPa) between 24 hr forecasts starting from initialized data sets and un-initialized input. For u, v and T, the statistics are for three dimensional domain. (DDFI - NOIN) : Changes induced by DDFI on NOIN input ; (RDFI - NOIN) : Changes made by RDFI scheme on NOIN fields and (RADF - NOIN) : changes made by RADF technique on NOIN data.

	RMS				MAXD			
	u	v	T	p_s	u	v	T	p_s
DDFI - NOIN	0.50	0.40	0.15	0.20	8.37	5.18	1.29	0.89
RDFI - NOIN	0.30	0.30	0.10	0.16	2.18	2. 61	0.92	0.69
RADF-NOIN	0.26	0.25	0.09	0.13	2.30	2.56	0.93	0.66

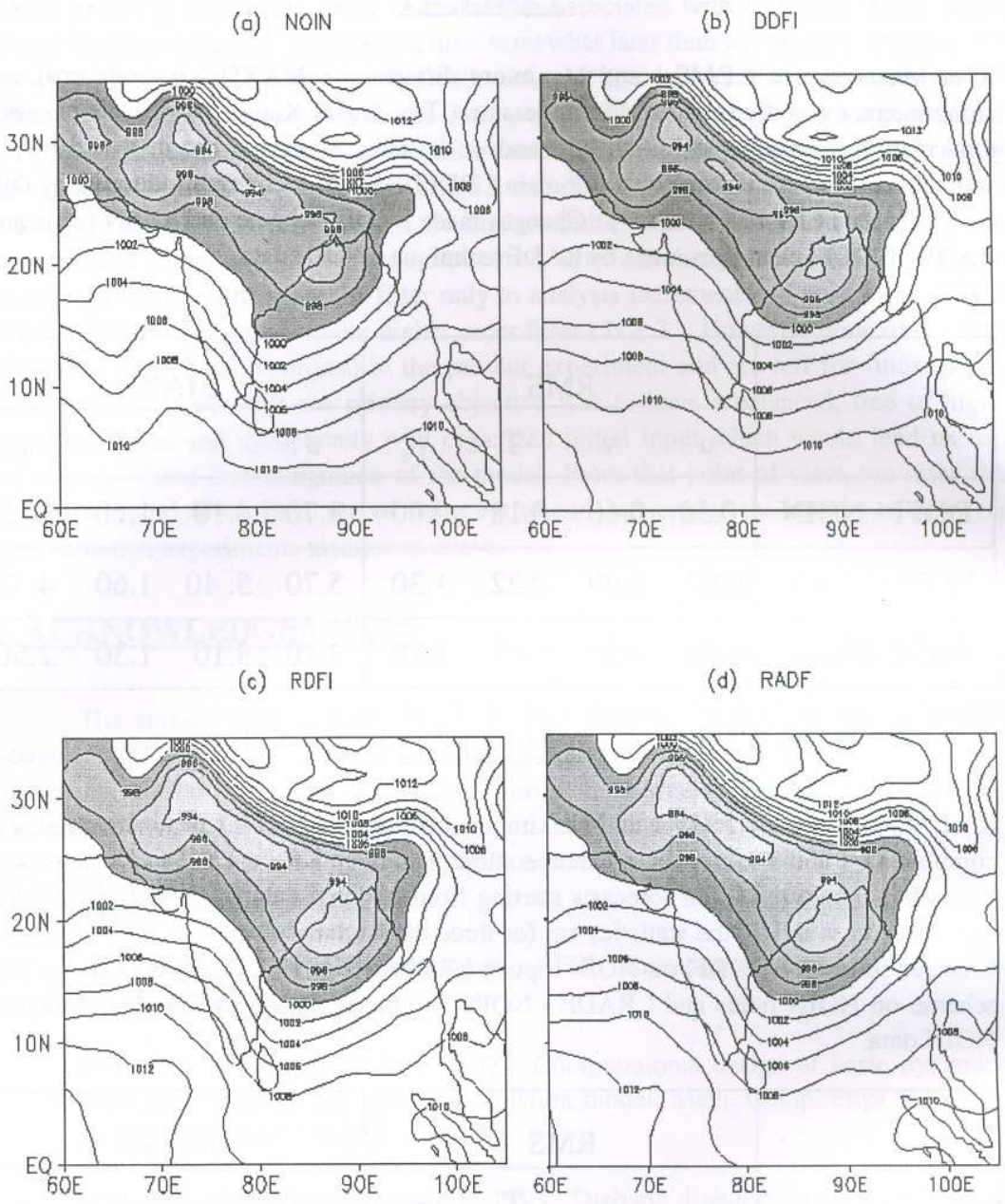

Figure 1 : Mean sea-level pressure (in hPa) maps at initial time (t=0) valid at 1200 UTC on 7 July, 1979. (a) NOIN case, (b) DDFI case, (c) RDFI case and (d) RADF case.

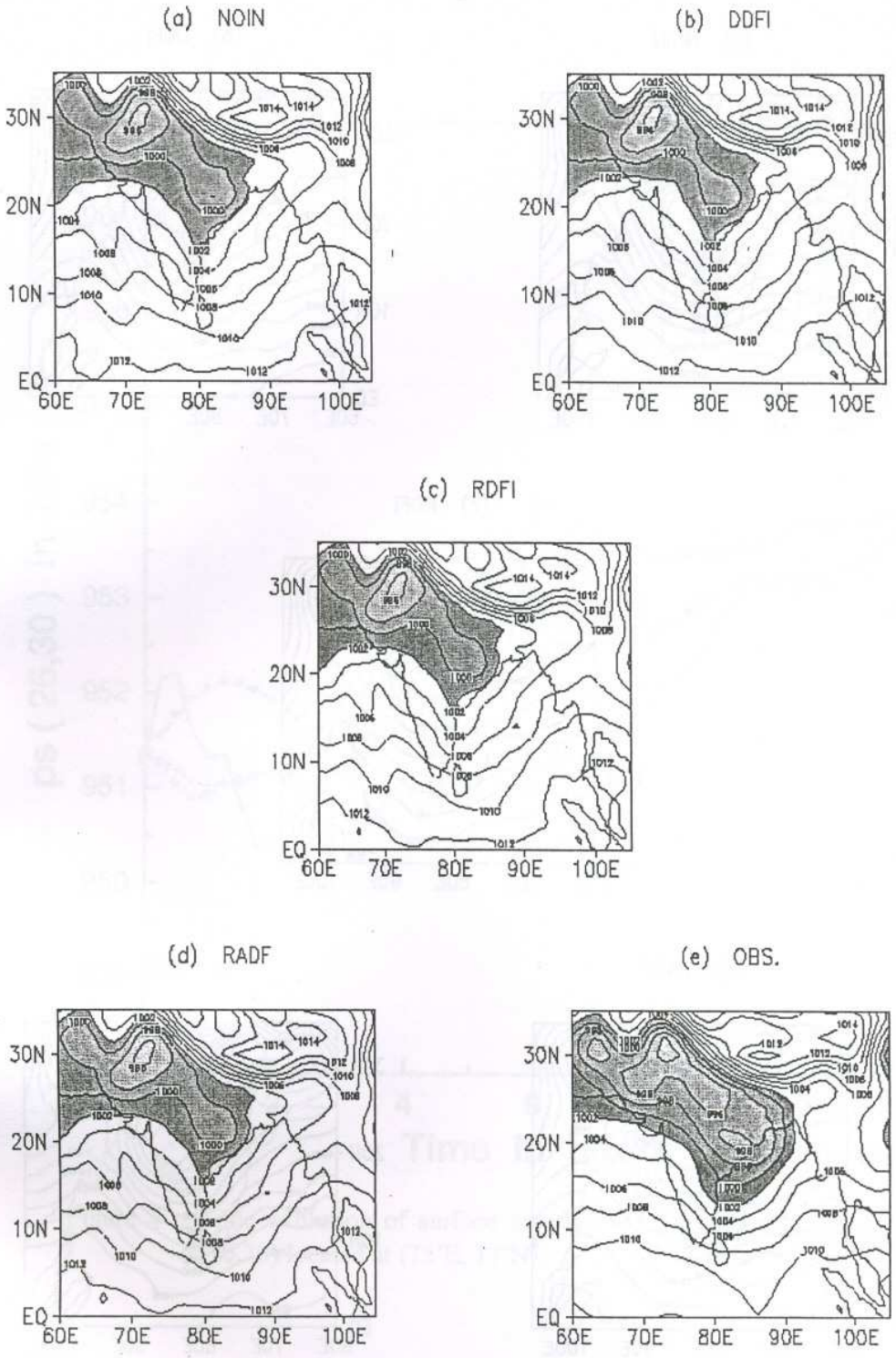

Figure 2 : 24 hr forecast mean sea-level pressure (in hPa) fields valid for 1200 UTC of 8 July, 1979 and corresponding verification chart. (a) NOIN case, (b) DDFI case, (c) RDFI case, (d) RADF case and (e) verification

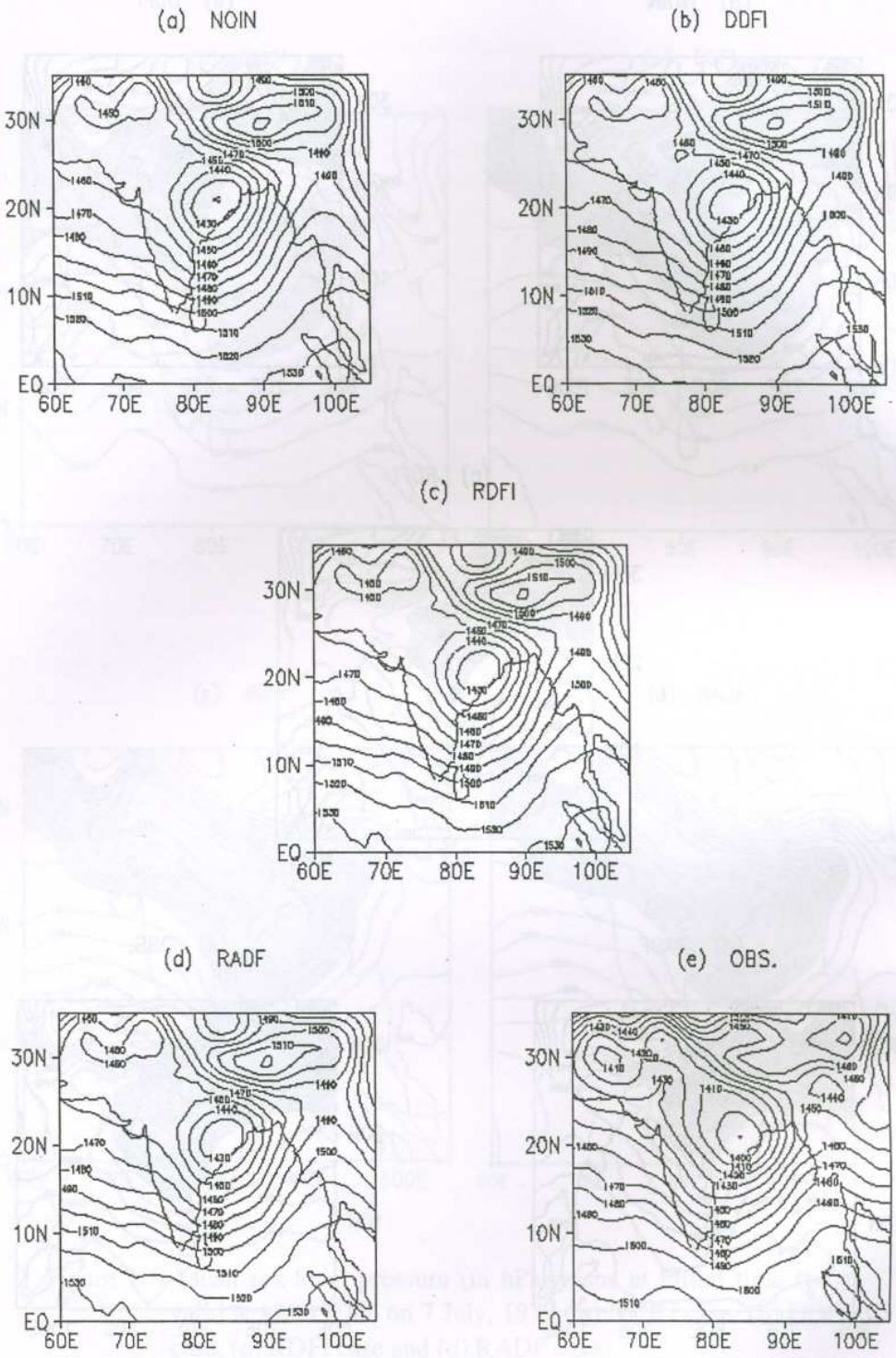

Figure 3 : 24 hr forecast geopotential height fields at 850 hPa level valid for 1200 UTC of 8 July, 1979 and corresponding verification chart. (a) NOIN case, (b) DDFI case, (c) RDFI case, (d) RADF case and (e) verification

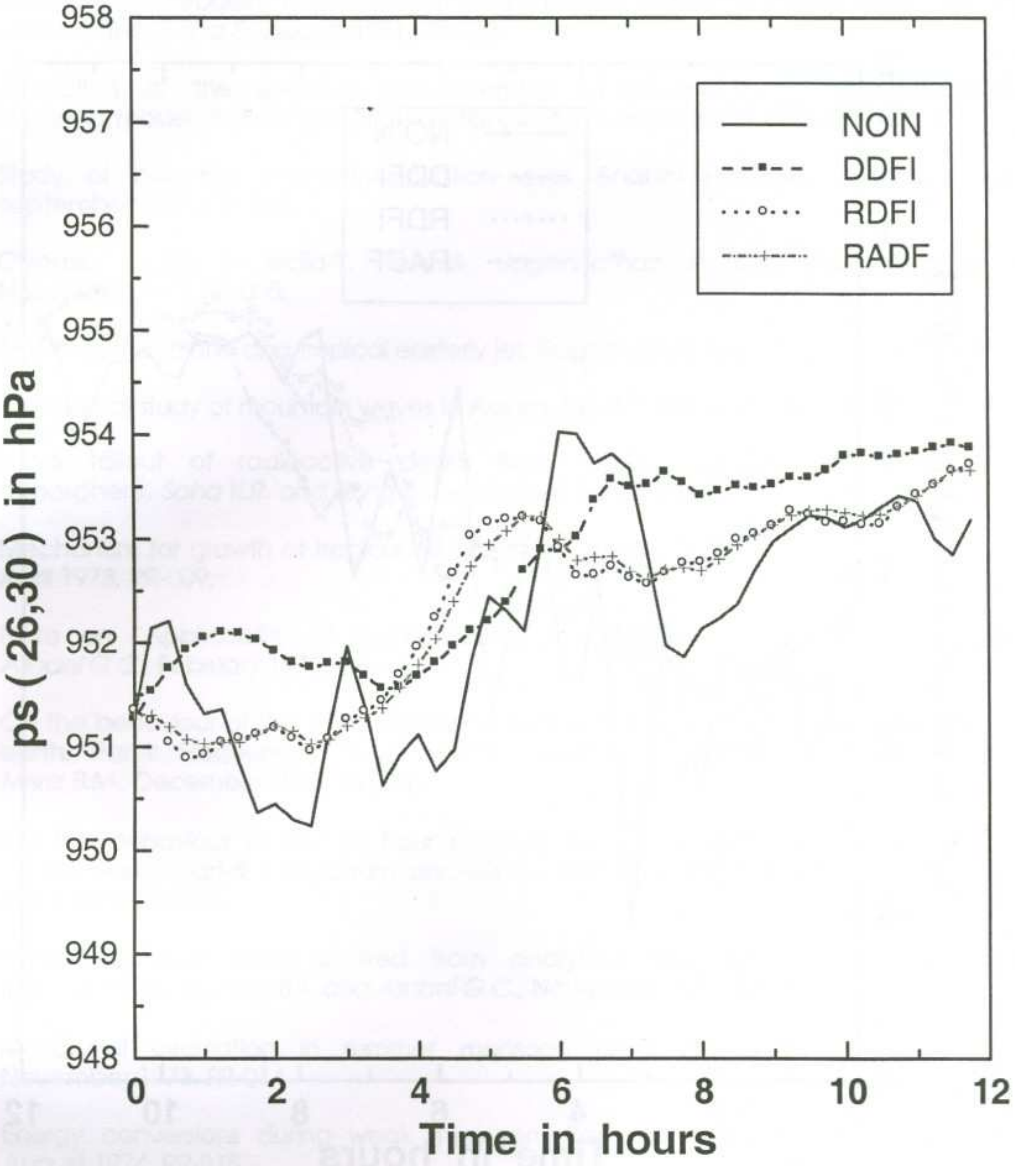

Figure 4 : Time evolution of surface pressure (ps) at a model grid point (26,30) located at (75°E, 17°N).

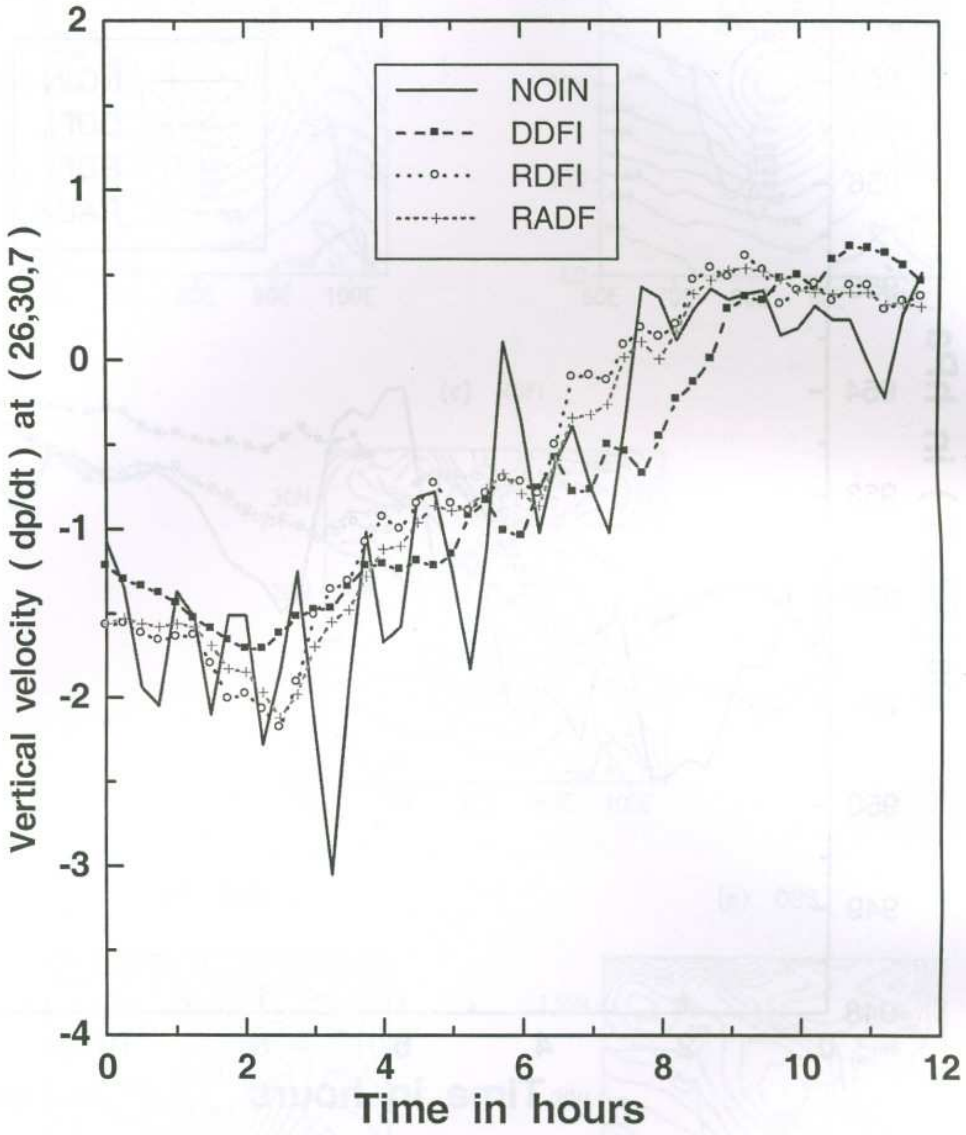

Figure 5 : Time evolution of 700 hPa level vertical velocity (dp/dt) in 10^{-3} hPa/sec at a model grid point (26,30,7) located over (75°E, 17°N).

I. I. T. M. RESEARCH REPORTS

- Energetic consistency of truncated models, *Asnani G.C.*, August 1971, RR-001.
- Note on the turbulent fluxes of heat and moisture in the boundary layer over the Arabian Sea, *Sinha S.*, August 1971, RR-002.
- Simulation of the spectral characteristics of the lower atmosphere by a simple electrical model and using it for prediction, *Sinha S.*, September 1971, RR-003.
- Study of potential evapo-transpiration over Andhra Pradesh, *Rakhecha P.R.*, September 1971, RR-004.
- Climatic cycles in India-1: Rainfall, *Jagannathan P. and Parthasarathy B.*, November 1971, RR-005.
- Tibetan anticyclone and tropical easterly jet, *Raghavan K.*, September 1972, RR-006.
- Theoretical study of mountain waves in Assam, *De U.S.*, February 1973, RR-007.
- Local fallout of radioactive debris from nuclear explosion in a monsoon atmosphere, *Saha K.R. and Sinha S.*, December 1972, RR-008.
- Mechanism for growth of tropical disturbances, *Asnani G.C. and Keshavamurty R.N.*, April 1973, RR-009.
- Note on "Applicability of quasi-geostrophic barotropic model in the tropics", *Asnani G.C.*, February 1973, RR-010.
- On the behaviour of the 24-hour pressure tendency oscillations on the surface of the earth, Part-I: Frequency analysis, Part-II: Spectrum analysis for tropical stations, *Misra B.M.*, December 1973, RR-011.
- On the behaviour of the 24 hour pressure tendency oscillations on the surface of the earth, Part-III : Spectrum analysis for the extra-tropical stations, *Misra B.M.*, July 1976, RR-011A.
- Dynamical parameters derived from analytical functions representing Indian monsoon flow, *Awade S.T. and Asnani G.C.*, November 1973, RR-012.
- Meridional circulation in summer monsoon of Southeast Asia, *Asnani G.C.*, November 1973, RR-014.
- Energy conversions during weak monsoon, *Keshavamurty R.N. and Awade S.T.*, August 1974, RR-015.
- Vertical motion in the Indian summer monsoon, *Awade S.T. and Keshavamurty R.N.*, August 1974, RR-016.
- Semi-annual pressure oscillation from sea level to 100mb in the northern hemisphere, *Asnani G.C. and Verma R.K.*, August 1974, RR-017.
- Suitable tables for application of gamma probability model to rainfall, *Mooley D.A.*, November 1974, RR-018.
- Annual and semi-annual thickness oscillation in thenorthern hemisphere, *Asnani G.C. and Verma R.K.*, January 1975, RR-020.

- Spherical harmonic analysis of the normal constant pressure charts in the northern hemisphere, *Awade S.T., Asnani G.C. and Keshavamurty R.N.*, May 1978, RR-021.
- Dynamical parameters derived from analytical function representing normal July zonal flow along 87.5 °E, *Awade S.T. and Asnani G.C.*, May 1978, RR-022.
- Study of trends and periodicities in the seasonal and annual rainfall of India, *Parthasarathy B. and Dhar O.N.*, July 1975, RR-023.
- Southern hemisphere influence on Indian rainfall, *Raghavan K.., Paul D.K. and Upasani P.U.*, February 1976, RR-024.
- Climatic fluctuations over Indian region - Rainfall : A review, *Parthasarathy B. and Dhar O.N.*, May 1978, RR-025.
- Annual variation of meridional flux of sensible heat, *Verma R.K. and Asnani G.C.*, December 1978, RR-026.
- Poisson distribution and years of bad monsoon over India, *Mooley D.A and Parthasarathy B.*, April 1980, RR-027.
- On accelerating the FFT of Cooley and Tukey, *Mishra S.K.*, February 1981, RR-028.
- Wind tunnel for simulation studies of the atmospheric boundary layer, *Sivaramakrishnan S.*, February 1981, RR-029.
- Hundred years of Karnataka rainfall, *Parthasarathy B. and Mooley D.A.*, March 1981, RR-030.
- Study of the anomalous thermal and wind patterns during early summer season of 1979 over the Afro-Asian region in relation to the large-scale performance of the monsoon over India, *Verma R.K. and Sikka D.R.*, March 1981, RR-031.
- Some aspects of oceanic ITCZ and its disturbances during the onset and established phase of summer monsoon studied with Monex-79 data, *Sikka D.R., Paul D.K. and Singh S.V.*, March 1981, RR- 032.
- Modification of Palmer drought index, *Bhalme H.N. and Mooley D.A.*, March 1981, RR-033.
- Meteorological rocket payload for Menaka-II/Rohini 200 and its developmental details, *Vernekar K.G. and Brij Mohan*, April 1981, RR-034.
- Harmonic analysis of normal pentad rainfall of Indian stations, *Anathakrishnan R. and Pathan J.M.*, October 1981, RR-035.
- Pentad rainfall charts and space-time variations of rainfall over India and the adjoining areas, *Anathakrishnan R. and Pathan J.M.*, November 1981, RR-036.
- Dynamic effects of orography on the large scale motion of the atmosphere Part I : Zonal flow and elliptic barrier with maximum height of one km., *Bavadekar S.N. and Khaladkar R.M.*, January 1983, RR-037.
- Limited area five level primitive equation model, *Singh S.S.*, February 1983, RR-038.
- Developmental details of vortex and other aircraft thermometers, *Vernekar K.G., Brij Mohan and Srivastava S.*, November 1983, RR-039.

- Note on the preliminary results of integration of a five level P.E. model with westerly wind and low orography, *Bavadekar S.N., Khaladkar R.M., Bandyopadhyay A. and Seetaramayya P.*, November 1983, RR-040.

- Long-term variability of summer monsoon and climatic change, *Verma R.K., Subramaniam K. and Dugam S.S.*, December 1984, RR-041.

- Project report on multidimensional initialization for NWP models, *Sinha S.*, February 1989, RR-042.

- Numerical experiments with inclusion of orography in five level P.E. Model in pressure-coordinates for interhemispheric region, *Bavadekar S.N. and Khaladkar R.M.*, March 1989, RR-043.

- Application of a quasi-lagrangian regional model for monsoon prediction, *Singh S.S. and Bandyopadhyay A.*, July 1990, RR-044.

- High resolution UV-visible spectrometer for atmospheric studies, *Bose S., Trimbake H.N., Londhe A.L. and Jadhav D.B.*, January 1991, RR-045.

- Fortran-77algorithm for cubic spline interpolation for regular and irregular grids, *Tandon M.K.*, November 1991, RR-046.

- Fortran algorithm for 2-dimensional harmonic analysis, *Tandon M.K.*, November 1991, RR- 047.

- 500 hPa ridge and Indian summer monsoon rainfall : A detailed diagnostic study, *Krishna Kumar K., Rupa Kumar K. and Pant G.B.*, November 1991, RR-048.

- Documentation of the regional six level primitive equation model, *Singh S.S. and Vaidya S.S.*, February 1992, RR-049.

- Utilisation of magnetic tapes on ND-560 computer system, *Kripalani R.H. and Athale S.U.*, July 1992, RR-050.

- Spatial patterns of Indian summer monsoon rainfall for the period 1871-1990, *Kripalani R.H., Kulkarni A.A., Panchawagh N.V. and Singh S.V.*, August 1992, RR-051.

- FORTRAN algorithm for divergent and rotational wind fields, *Tandon M.K.*, November 1992, RR-052.

- Construction and analysis of all-India summer monsoon rainfall series for the longest instrumental period: 1813-1991, *Sontakke N.A., Pant G.B. and Singh N.*, October 1992, RR-053.

- Some aspects of solar radiation, *Tandon M.K.*, February 1993, RR-054.

- Design of a stepper motor driver circuit for use in the moving platform, *Dharmaraj T. and Vernekar K.G.*, July 1993, RR-055.

- Experimental set-up to estimate the heat budget near the land surface interface, *Vernekar K.G., Saxena S., Pillai J.S., Murthy B.S., Dharmaraj T. and Brij Mohan*, July 1993, RR-056.

- Identification of self-organized criticality in atmospheric total ozone variability, *Selvam A.M. and Radhamani M.*, July 1993, RR-057.

- Deterministic chaos and numerical weather prediction, *Selvam A.M.*, February 1994, RR-058.

- Evaluation of a limited area model forecasts, *Singh S.S., Vaidya S.S Bandyopadhyay A., Kulkarni A.A, Bawiskar S.M.,Sanjay J., Trivedi D.K. and Iyer U.*, October 1994, RR-059.

- Signatures of a universal spectrum for atmospheric interannual variability in COADS temperature time series, *Selvam A.M., Joshi R.R. and Vijayakumar R.*, October 1994, RR-060.

- Identification of self-organized criticality in the interannual veriability of global surface temperature, *Selvam A.M. and Radhamani M.*, October 1994, RR-061.

- Identification of a universal spectrum for nonlinear veriability of solar-geophysical parameters, *Selvam A.M., Kulkarni M.K., Pethkar J.S. and Vijayakumar R.*, October 1994, RR-062.

- Universal spectrum for fluxes of energetic charged particles from the earth's magnetosphere, *Selvam A.M. and Radhamani M.*, June 1995, RR-063.

- Estimation of nonlinear kinetic energy exchanges into individual triad interactions in the frequency domain by use of the cross-spectral technique, *Chakraborty D.R.*, August 1995, RR-064.

- Monthly and seasonal rainfall series for all-India homogeneous regions and meteorological subdivisions: 1871-1994, *Parthasarathy B., Munot A.A. and Kothawale D.R.*, August 1995, RR-065.

- Thermodynamics of the mixing processes in the atmospheric boundary layer over Pune during summer monsoon season, *Morwal S.B. and Parasnis S.S.*, March 1996, RR-066.

- Instrumental period rainfall series of the Indian region: A documentation, *Singh N. and Sontakke N.A.*, March 1996, RR-067.

- Some numerical experiments on roundoff-error growth in finite precision numerical computation, *Fadnavis S.*, May 1996, RR-068.

- Fractal nature of MONTBLEX time series data, *Selvam A.M. and Sapre V.V.*, May 1996, RR-069.

- Homogeneous regional summer monsoon rainfall over India: Interannual variability and teleconnections, *Parthasarathy B., Rupa Kumar K. and Munot A.A.*, May 1996, RR-070.

- Universal spectrum for sunspot number variability, *Selvam A.M. and Radhamani M.*, November 1996, RR-071.

- Development of simple reduced gravity ocean model for the study of upper north Indian ocean, *Behera S.K. and Salvekar P.S.*, November 1996, RR-072.

- Study of circadian rhythm and meteorological factors influencing acute myocardial infraction, *Selvam A.M., Sen D. and Mody S.M.S.*, April 1997, RR-073.

- Signatures of universal spectrum for atmospheric gravity waves in southern oscillation index time series, *Selvam A.M., Kulkarni M.K., Pethkar J.S. and Vijayakumar R.*, December 1997, RR-074.

- Some example of X-Y plots on Silicon Graphics, *Selvam A.M., Fadnavis S. and Gharge S.P.*, May 1998, RR-075.

- Simulation of monsoon transient disturbances in a GCM, *Ashok K., Soman M.K. and Satyan V.*,August 1998, RR-076.

- Universal spectrum for intraseasonal variability in TOGA temperature time series, *Selvam A.M., Radhamani M., Fadnavis S. and Tinmaker M.I.R.*, August 1998, RR-077.

- One dimensional model of atmospheric boundary layer, *Parasnis S.S., Kulkarni M.K., Arulraj S. and Vernekar K.G.*, February 1999, RR-078.

- Diagnostic model of the surface boundary layer - A new approach, *Sinha S.*, February 1999, RR-079.

- Computation of thermal properties of surface soil from energy balance equation using force - restore method, *Sinha S.*, February 1999, RR-080.

- Fractal nature of TOGA temperature time series, *Selvam A.M. and Sapre V.V.*, February 1999, RR-081.

- Evolution of convective boundary layer over the Deccan Plateau during summer monsoon, *Parasnis S.S.*, February 1999, RR-082.

- Self-organized criticality in daily incidence of acute myocardial infarction, *Selvam A.M., Sen D., and Mody S.M.S.*, Feburary 1999, RR-083.

- Monsoon simulation of 1991 and 1994 by GCM : Sensitivity to SST distribution, *Ashrit R.G., Mandke S.K. and Soman M.K.*, March 1999, RR-084.

- Numerical investigation on wind induced interannual variability of the north Indian Ocean SST, *Behera S.K., Salvekar P.S. and Ganer D.W.*, April 1999, RR-085.

- On step mountain eta model, *Mukhopadhyay P., Vaidya S.S., Sanjay J. and Singh S.S.*, October 1999, RR-086.

- Land surface processes experiment in the Sabarmati river basin: an overview and early results, *Vernekar K.G., Sinha S., Sadani L.K., Sivaramakrishnan S., Parasnis S.S., Brij Mohan, Saxena S., Dharamraj T., Pillai, J.S., Murthy B.S., Debaje, S.B., Patil, M.N. and Singh A.B.*, November 1999, RR-087.

- Reduction of AGCM systematic error by Artificial Neural Network: A new approach for dynamical seasonal prediction of Indian summer monsoon rainfall, *Sahai A.K. and Satyan V.*, December 2000, RR-088.

- Ensemble GCM simulations of the contrasting Indian summer monsoons of the 1987 and 1988, *Mujumdar M.* and *Krishnan R.*, February 2001, RR-089.

- Aerosol measurements using lidar and radiometers at Pune during INDOEX field phases, *Maheskumar R.S., Devara P.C.S., Raj P.E., Jaya Rao Y.,Pandithurai G., Dani K.K., Saha S.K., Sonbawne S.M. and Tiwari Y.K.*, December 2001, RR-090.

- Modelling studies of the 2000 Indian summer monsoon and extended analysis, *Krishnan R., Mujumdar M., Vaidya V., Ramesh K.V. and Satyan V.*, December 2001, RR-091.

- Intercomparison of Asian summer monsoon 1997 simulated by atmospheric general circulation models, *Mandke S.K., Ramesh K.V. and Satyan V.*, December 2001, RR-092.

- Prospects of prediction of Indian summer monsoon rainfall using global SST anomalies, *Sahai A.K, Grimm A.M., Satyan V. and Pant G.B.*, April 2002, RR-093.

- Estimation of nonlinear heat and momentum transfer in the frequency domain buy the use of frequency co-spectra and cross-bispectra, *Chakraborty D.R. and Biswas M.K.*, August 2002, RR-094

- Real time simulations of surface circulations by a simple ocean model, *P Rahul Chand Reddy, Salvekar P.S., Ganer D.W. and Deo A.A.*, January 2003, RR-095

- Evidence of twin gyres in the Indian ocean : new insights using reduced gravity model by daily winds, *P Rahul Chand Reddy, Salvekar P.S., Ganer D.W. and Deo A.A.*, February 2003, RR-096

- Dynamical seasonal prediction experiments of the Indian summer monsoon, *Milind Mujumdar, R. Krishnan and V. Satyan*, June 2003, RR-097

- Thermodynamics and dynamics of the upper ocean mixed layer in the central and eastern Arabian sea, *C. Gnanaseelan, A.K. Mishra, Bijoy Thompson and P.S. Salvekar*, August 2003, RR-098

- Measurement of profiles and surface energy fluxes on the west coast of India at Vasco-Da-Gama, Goa during ARMEX 2002-03, *S. Sivaramakrishnan, B.S. Murthy, T. Dharmaraj, Cini Sukumaran and T. Rajitha Madhu Priya*, August 2003, RR-099

- Time-mean oceanic response and interannual variability in a global ocean GCM simulation, *K.V. Ramesh and R. Krishnan*, September 2003, RR-100

- Multimodel scheme for prediction of monthly rainfall over India, *J.R. Kulkarni, Savita G. Kulkarni, Yogesh Badhe, Sanjeev S. Tambe, Bhaskar D. Kulkarni and G.B. Pant*, December 2003, RR-101

- Mixed-layer and thermocline interactions associated with monsoonal forcing over the Arabian sea, *R. Krishnan and K.V. Ramesh*, January 2004, RR-102

- Interannual variability of Kelvin and Rossby waves in the Indian ocean from topex/Poseidon altimetry data, *C. Gnanaseelan, B.H. Vaid, Paulo S. Polito and P.S. Salvekar*, March 2004, RR-103